Experimental Characterization of Electron-Beam-Driven Wakefield Modes in a Dielectric-Woodpile Cartesian Symmetric Structure

P. D. Hoang, G. Andonian, I. Gadjev, B. Naranjo, Y. Sakai, N. Sudar, O. Williams, M. Fedurin, K. Kusche, C. Swinson, P. Zhang, and J. B. Rosenzweig

Phys. Rev. Lett. **120**, 164801 — Published 19 April 2018

DOI: 10.1103/PhysRevLett.120.164801

Experimental characterization of electron beam driven wakefield modes in a dielectric woodpile Cartesian symmetric structure

P.D.Hoang,[1,*] G.Andonian,[1] I.Gadjev,[1] B.Naranjo,[1] Y.Sakai,[1] N.Sudar,[1]
O.Williams,[1] M.Fedurin,[2] K.Kusche,[2] C.Swinson,[2] P.Zhang,[3] and J.B.Rosenzweig[1]

[1]*Department of Physics and Astronomy, University of California, Los Angeles, California 90095-1547, USA*
[2]*Accelerator Test Facility, Brookhaven National Laboratory, Upton, NY 11973, USA*
[3]*School of Physical Electronics, University of Electronic Science and Technology of China, Chengdu, 610054, China*

(Dated: March 5, 2018)

Photonic structures operating in the terahertz (THz) spectral region enable the essential characteristics of confinement, modal control, and electric field shielding for very high gradient accelerators based on wakefields in dielectrics. We report here an experimental investigation of THz wakefield modes in a 3D photonic woodpile structure. Selective control in exciting or suppressing of wakefield modes with non-zero transverse wave vector is demonstrated by using drive beams of varying transverse ellipticity. Additionally, we show that the wakefield spectrum is insensitive to the offset position of strongly elliptical beams. These results are consistent with analytic theory and 3D simulations, and illustrate a key advantage of wakefield systems with Cartesian symmetry, the suppression of transverse wakes by elliptical beams.

PACS numbers: 41.60.Bq, 41.75.Ht, 42.70.Qs, 29.27.-a, 87.56.bd
Keywords: Dielectric Wakefield Acceleration, Transverse Wakefield, Coherent Cherenkov Radiation, Woodpile Photonic Crystal

Dielectric wakefield accelerators (DWA) driven by short-pulse, intense charged particle beams have recently emerged in the THz frequency regime [1]. In this burgeoning class of advanced accelerator, fields orders of magnitude beyond the current state of the art in radio-frequency (RF) linear accelerators – to greater than the GV/m level – are obtained. This progress is due in part to the availability of high-brightness, ultra-short pulse electron beams, and also to advances in few-micron resolution fabrication techniques. Recent experimental results on DWA using cylindrical dielectric lined waveguides have demonstrated sustained average accelerating gradients in excess of 1.3 GeV/m as reported in [2]. Attaining fields in an accelerator based on solid state matter in this spectral range is a significant achievement for advanced acceleration techniques. However, many further aspects of the DWA need to be experimentally addressed to bring the viability of the DWA methods toward promising applications, e.g. in future linear colliders [3] and compact light sources [4].

Even before the onset of dielectric breakdown [1], the upper bound of useful acceleration gradient is limited by high field phenomena in the dielectric material [2, 5]. To minimize these deleterious effects, the penetration of strong electric field into the dielectric from both the intense beam's space-charge fields and the electromagnetic mode excited in the beam's wake must be suppressed. Further, aside from materials considerations, one typically seeks to increase the DWA gradient by using a smaller aperture size, a, following the (Cherenkov) scaling $E_z \propto Q/a^2$ [6, 7]. However, transverse wakefields, which can cause spurious collective transverse motion that leads to beam breakup (BBU) instabilities, scale as $E_\perp \propto Q/a^3$, and thus beam stability at THz frequencies presents a formidable challenge [8]. One promising solution for mitigating transverse wakefields uses structures that possess aspects of Cartesian instead of cylindrical symmetry, with one dimension (x) having variations in the accelerating modes that are small on the scale of the mode wavelength. In the limit of highly elliptical $\sigma_x >> \sigma_y$ beams in a wide (in x) structure, the transverse wakefields diminish as $\vec{F}_\perp \propto 1/\sigma_x^2$ [6]. This potent BBU mitigation strategy requires more charge, distributed in an elliptical beam to drive the desired longitudinal wake, $E_z \propto Q/\sigma_x$. Given the stronger scaling of transverse-to-longitudinal coupling as $1/\sigma_x$, this approach allows GV/m accelerating wakes in a THz DWA, while controlling BBU.

While progress has been made in demonstrating mode excitation and concomitant acceleration of charge in slab-symmetric DWAs [9, 10], issues remain experimentally unaddressed. These include, in addition to demonstration of the suppression of transverse wakefields causing BBU, the mitigation of high field penetration into the dielectric that leads to nonlinear effects. The solution to the former may be approached by two key design features. First, one may do away with the flat longitudinal vacuum/dielectric interface present in the simple slab case, which enforces continuity of E_z, and achieve a field reduction in the dielectric by a factor as large as $1/\epsilon$ through the implementation of more appropriate boundary conditions. Photonic structures can be further used to confine modes within the accelerating vacuum channel. An example was demonstrated in [11] where a pair of 1D photonic Bragg reflectors were used to confine the modes formed between the slabs. Use of higher dimensional pho-

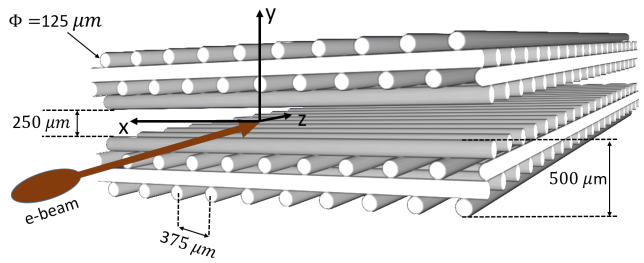

FIG. 1. (Color online) Computer rendered model of the woodpile structure with relevant dimensions.

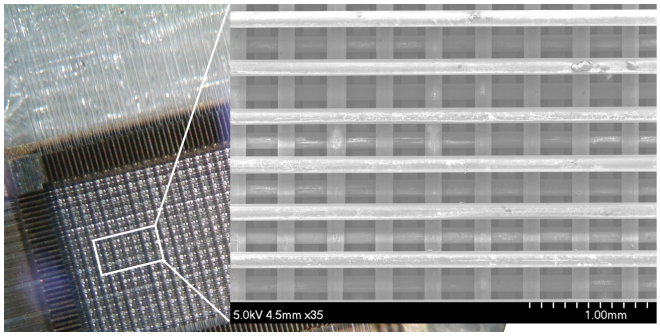

FIG. 2. (Color online) Optical image of sapphire rods in slotted holder during the manual fabrication process. Inset shows an SEM image (top down view) of a section of the device.

tonic structures having more sophisticated shapes can offer further capabilities for tuning mode properties [12], and controlling the variation of the field in all directions, potentially placing spurious modes outside of the band gap, permitting them to propagate away from the beam [13], and yielding a mode optimized for acceleration applications. On the other hand, the key solution to suppression of deleterious wakefield modes, including transverse (dipole-like) wakefields with large transverse wave number k_x which enable BBU instability, is the combination of Cartesian-symmetric structures and highly elliptical beam.

In this Letter, we therefore present a wakefield study of a structure having Cartesian symmetry properties, constituted of discrete, periodic dielectric rods that are formed into a so-termed woodpile [14, 15] geometry, schematically shown in Fig. 1. The introduction of the woodpile lattice into this symmetry class marks the first time that a 3D photonic crystal is incorporated into a THz DWA structure. The single-period woodpile structure studied here has relatively simple and well-known photonic properties and contains all basic modal ingredients from which more sophisticated structures can be understood. Our goal here is thus to experimentally demonstrate control over excitation of wakefield modes.

The features of the structure can be seen in Fig. 1. The structure is constructed of sapphire (Al_2O_3) rods. Each sapphire rod is 125 μm in diameter. Sapphire has long been a candidate for sub-mm DWA applications due to its mechanical robustness, high damage threshold [16], low loss, and a relatively high THz range dielectric constant ($\epsilon \approx 10.5$) [17]. Each of the two identical halves that makes up the structure consists of a full single woodpile stacking period [15, 18]. As seen in Fig. 1, the main periodicity in both the wide transverse x- and the longitudinal z-direction is 375 μm, and the vacuum gap that the beam traverses has a vertical clearance of 250 μm. The rods in the two rafts that are immediately below and above the drive beam run perpendicular to the beam axis, an orientation that serves to suppress electric field penetration into the dielectric while augmenting the longitudinal component of field in the defect region. There are 28 of these periods in the z-direction, equivalent to a length of 10.5 mm, and 16 in the x-direction, equivalent to 6 mm, in total. The structure was fabricated layer-by-layer (Fig. 2) using a holder with precision machined slots to facilitate the intricate arrangement.

Unlike the simple slab DWAs whose normal modes (LSE/LSM) can be solved for analytically [19–22], the woodpile is more sophisticated and requires numerical methods to obtain its modal structure $\omega(\vec{k})$. Wakefield modes driven by relativistic electrons ($|\vec{v}_e| = c$) are excited when the Cherenkov condition [23], $\omega(\vec{k}_\perp, k_z) = ck_z$, is met, where for clarity, the wave vector has been separated into its longitudinal and transverse components. While a point-like beam can excite all possible modes, we can limit coupling to large wave vectors by tailoring the Fourier content of the beam. For example, by adjusting the beam bunch length, σ_z, we can select the highest k_z. Similarly, the beam width, σ_x, directly affects the contribution of k_x to the wakefield spectrum ($k_x \propto 1/\sigma_x$). This control over k_x has a particular ramification in short range single bunch BBU instability where a large wave number can filament (flute) the distribution of charge in x. As noted above excitation of transverse, dipole-like wakes which are responsible for long range multibunch beam breakup is also mitigated by having a large beam width [6]. It is seen that a DWA with Cartesian geometry offers critical advantages over cylindrical structures, by breaking the unfavorable scaling of transverse-to-longitudinal wake coupling.

As the major emphasis of the presented experiments on the woodpile is an examination of the wakefield frequency spectrum, to orient the reader to the salient aspects of this photonic structure, we first introduce a computational analysis of the modes that can be excited via the wakefield mechanism. We begin by examining first the structure's frequency domain properties, and review the computational investigation of the most important structure eigenmodes. To perform this analysis [24], shown in Fig. 3, we make the following simplifications. First, we assume that the eigenmodes of the real finite structure are similar to those of an infinite (in x-z plane) but oth-

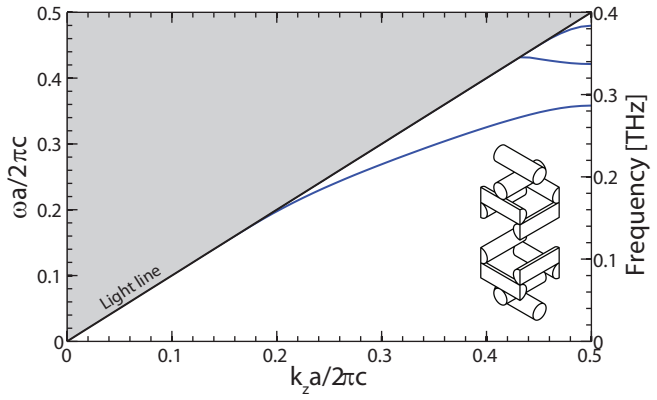

FIG. 3. (Color online) Woodpile structure dispersion showing three symmetric accelerating bands as a function of normalized longitudinal (z) wave vector. Wakefield modes are formed where the light line meets the bands, $\omega(k_z) = ck_z$. Left (right) vertical axis shows normalized (real) frequency; a is the periodicity of the structure and is 375 μm. The inset shows the unit cell used for the eigenmode calculation.

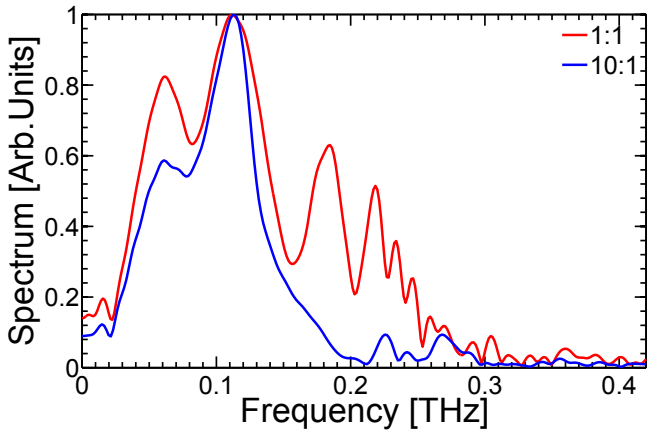

FIG. 4. (Color online) FDTD simulations, using experimental beam parameters, showing normalized spectra for varying beam ellipticity σ_x:σ_y (1:1, 10:1). For both simulations, the beams propagate symmetrically through the structure and have $\sigma_y = 50$ μm and $\sigma_z = 250\mu$m.

erwise equivalent structure. This assumption affords use of the simple unit cell shown in the inset of Fig. 3, thus avoiding the complications related to the use of a full super cell. Second, to emphasize first the dominant accelerating modes, particularly those preferentially excited by strongly elliptical $\sigma_x/\sigma_y \gg 1$ beams, we restrict our attention only to the eigenmodes with purely longitudinal wave vector, $\vec{k} = k_z\hat{z}$, and all other transverse components of $\vec{k}$ are set to zero. Third, we further restrict the eigenmodes to only even symmetry (accelerating modes) defined as follows. The woodpile possesses two mirror symmetry planes ($x = 0$ and $y = 0$) where $\epsilon(\vec{r}) = \epsilon(\mathcal{M}\cdot\vec{r})$, and the mirror operator acting on a vector is defined as $\mathcal{M}_x \cdot \langle x, y, z\rangle = \langle -x, y, z\rangle$ and $\mathcal{M}_y \cdot \langle x, y, z\rangle = \langle x, -y, z\rangle$.

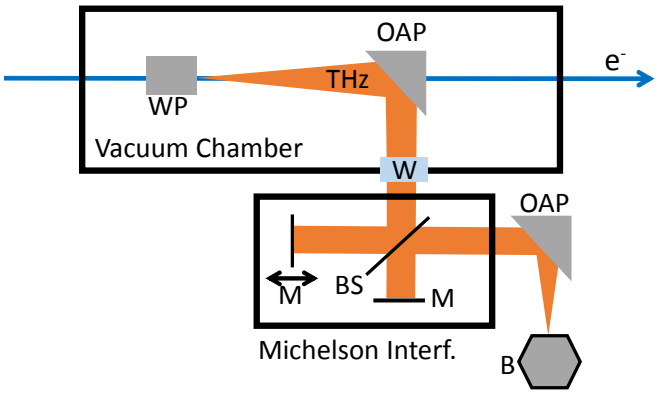

FIG. 5. (Color online) Schematic of the experiment. An electron bunch generates Cherenkov radiation as it travels through the woodpile structure (WP). The THz pulse is launched from the structure, and collimated by an off-axis parabolic mirror (OAP). The pulse passes through a THz-transmissive window (W) to a Michelson interferometer. In the interferometer, the THz pulse is split by a beam splitter (BS) and recombined at the detector (B) as a function of pulse delay from a translatable mirror (M).

For modes propagating in the z-direction, the field is either even (+) or odd (−), $\mathcal{M}_i \cdot \vec{E}(\mathcal{M}_i \cdot \vec{r}) = \pm\vec{E}(\vec{r})$ where $i = x, y$. A symmetric mode is even under both mirror reflections. As we shall see momentarily, these assumptions are justified for drive beams with a large aspect ratio which are the appropriate choice for this type of structures.

To demonstrate all these effects, and their manifestation as detectable changes to the wakefield spectrum, we have performed beam driven wakefield simulations in a finite-difference time-domain (FDTD) package [25, 26]. Here both the beam and the structure are modeled using parameters resembling those in the experiments. In Fig. 4, which shows the transmitted wakefield spectrum through a plane placed outside the structure, it is clear that the complexity of the wakes excited by the round aspect ratio beam (1:1) is reduced significantly by the use of a highly elliptical (10:1) beam. Using the dispersion of Fig. 3 as a guide, we identify the highest peak in the spectra of the wakes as the fundamental accelerating mode. All other peaks which are prominent in the wake spectrum excited by the round aspect ratio beam are attributable to the presence of modes with $k_x \neq 0$. This is concluded because they are too low in frequency to be identified with the next two higher order modes in Fig. 3 which only occur $\gtrsim 350$ GHz.

The simulation exercise shown in Fig. 3 and Fig. 4 suggest a set of design tools for wakefield modes. For example, one can select the frequency of the fundamental accelerating mode by choosing a, the structure's periodicity (375 μm in this case), and corresponding bunch length σ_z to ensure such mode is excited. An appropriate

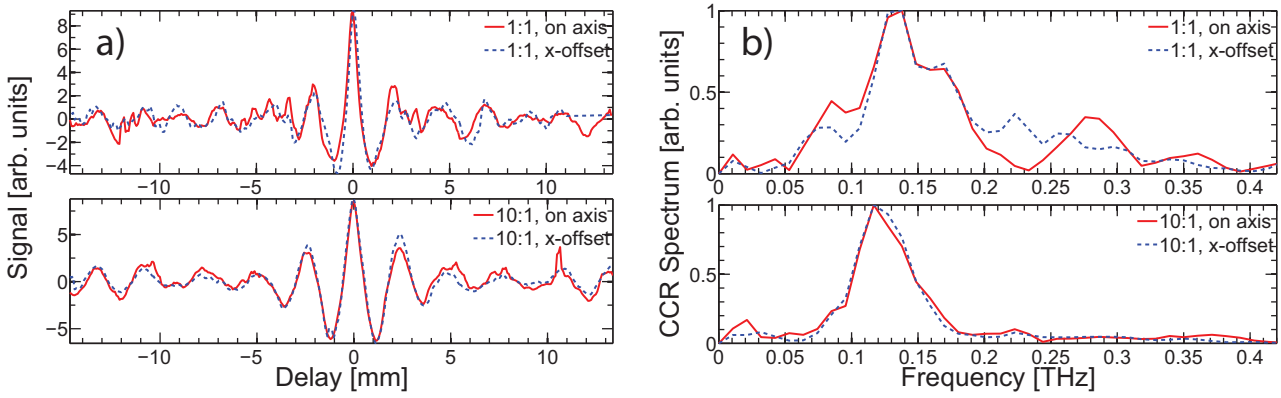

FIG. 6. (Color online) **a)** (Left two panels) Field autocorrelation or interferograms of the CCR signals measured by using Michelson interferometry. The labels, 1:1 (top panel) and 10:1 (bottom panel), refer to the ratio σ_x/σ_y, where $\sigma_y = 50$ μm. The x-offset is 1 mm. **b)** (Right two panels) The corresponding wakefield spectra obtained by Fourier transforming the interferograms in a).

(preferably large) σ_x further tailors the wakefield content by eliminating the presence of high wave number k_x.

The effect of beam ellipticity on the wake spectrum is demonstrated in a set of experiments conceptually similar to the scenario shown in simulations. That is, we measured the spectral content of the wakes for a round and elliptical aspect ratio beams. The main component of the diagnostics suite is a Michelson interferometer, a well-known technique [27] which has been adapted for THz wakefield spectral characterization [9, 11, 28]. The experimental setup is shown schematically in Fig. 5. At the Brookhaven National Laboratory Accelerator Test Facility (BNL ATF), where the experiment was carried out, 57.6 MeV electrons bunches having normalized emittance ϵ_n =2mm-mrad were focused to desired transverse beam sizes and waist location by a set of quadrupole magnets. The beam aspect ratio, σ_x/σ_y, was measured by fitting its size on four beam profile monitors in the drift section downstream of the final magnetic focusing element. For the results presented in this article, two beam transverse ratios were established, 1:1 and 10:1. We refer to these cases as round and elliptical beams, respectively.

To ensure passage of the beam through the structure, the beam vertical size at the waist was set to $\sigma_y \approx 50$ μm. A Faraday cup located downstream of the structure was used to ensure minimal beam loss due to scraping. It was determined that $\sim 10\%$ of charge was lost to the structure for both cases, and that on average the round and elliptical beam contained 150 pC and 235 pC of charge respectively. We note here that the difference in charge does not affect our results, as charge only contributes to the magnitude of the field and not its frequency content, which is set by the bunch length σ_z. Here, we required $\sigma_t = \sigma_z/c$ to be sub-picosecond to ensure the coherent excitation of THz modes, and employed coherent diffraction radiation (CDR) [29] to non-destructively characterize it. A 2.5 mm aperture was used to generate CDR whose duration was measured using the Michelson interferometer. By direct fitting [30] it was established that $\sigma_z \approx 250$ μm ($\sigma_t \approx 0.83$ psec). This dimension was checked, and its invariance determined, independent of transverse ellipticity, thus guaranteeing that the beams always accesses the same spectral region, and that any differences in the wakefield are only due to changing of σ_x.

In Fig. 6, we show the measured interferograms (a) and their corresponding spectra (b) where we see again the effects seen in Fig. 4. Namely, the elliptical beam preferentially couples only to the fundamental accelerating mode and remains so even when an x-offset of 1 mm is introduced. In contrast, the content of the wakefield spectrum driven by the round beam is much more complex and displays some degree of sensitivity to x-offset as manifested by the small change in the spectrum. This is expected as the round beam is spatially ($\sigma_x = \sigma_y = 50$ μm) smaller than the periodicity of the structure (375 μm) and thus can probe variation of the field along the direction of displacement. The small difference in the wakefield spectrum excited by the displaced round beam can also be interpreted as the presence of x-dipole modes which exist and may contribute to the complex BBU behavior. The more dominant y-dipole modes, which are associated with a y-offset, cannot be probed directly with the current setup as the narrow vacuum gap prevented us from translating the beam in this direction without encountering the structure. Nonetheless, theoretical analysis and simulations indicate that an elliptical aspect ratio beam similarly have negligible coupling to them.

In summary, we have investigated properties of THz wakefields in a Cartesian dielectric woodpile. By observing the wakefield spectrum while changing the beam width and position, we have demonstrated control of mode excitation. We found that a high aspect ratio ($\sigma_x/\sigma_y >> 1$) beam preferentially couples to purely longitudinal wave vector modes. Furthermore, the wakefield

spectrum driven by such beam was robust to displacement, in stark contrast to the spectrum driven by a similar σ_y beam having aspect ratio near unity. The results corroborated by numerical simulations confirm a theoretical prediction and have a significant impact toward resolving the outstanding problem of beam breakup instabilities. Building upon this work, more preparation is under way for an experimental investigation of a full-fledged 3D photonic DWA structure with a complete band gap for high gradient field confinement. Our preliminary calculations show that using the proposed FACET II [31] parameters and a 10:1 beam as a start, the accelerating gradient may exceed 2 GeV/m. Such experiments will also critically permit exploration of suppression of field penetration into the dielectric.

We thank Dr. Stanislav Baturin of the University of Chicago for important discussions. This work supported by the US DOE contract DE-SC0009914, and US Dept. of Homeland Security Grant 2014-DN-077-ARI084-01. Student stipend was partially provided by Office of Science Graduate Student Research (SCGSR) program. This research used resources of the Brookhaven National Laboratory Accelerator Test Facility, which is a DOE Office of Science user facility.

* hoangpd@g.ucla.edu

[1] M. Thompson, H. Badakov, A. Cook, J. Rosenzweig, R. Tikhoplav, G. Travish, I. Blumenfeld, M. Hogan, R. Ischebeck, N. Kirby, *et al.*, Phys. Rev. Lett. **100**, 214801 (2008).

[2] B. D. O'Shea, G. Andonian, S. K. Barber, K. L. Fitzmorris, S. Hakimi, J. Harrison, P. D. Hoang, M. J. Hogan, B. Naranjo, O. B. Williams, V. Yakimenko, and J. B. Rosenzweig, Nat. Commun. **7**, 12763 (2016).

[3] B. Barish, N. Walker, and H. Yamamoto, Sci. Am. **298**, 54 (2008).

[4] P. Emma, R. Akre, J. Arthur, R. Bionta, C. Bostedt, J. Bozek, A. Brachmann, P. Bucksbaum, R. Coffee, F.-J. Decker, *et al.*, Nat. Photon. **4**, 641 (2010).

[5] K. Dolgaleva, D. V. Materikina, R. W. Boyd, and S. A. Kozlov, Physical Review A **92**, 023809 (2015).

[6] A. Tremaine, J. Rosenzweig, and P. Schoessow, Phys. Rev. E **56**, 7204 (1997).

[7] N. Barov, J. B. Rosenzweig, M. E. Conde, W. Gai, and J. G. Power, Phys. Rev. ST Accel. Beams **3**, 011301 (2000).

[8] C. Li, W. Gai, C. Jing, J. G. Power, C. X. Tang, and A. Zholents, Phys. Rev. ST Accel. Beams **17**, 091302 (2014).

[9] G. Andonian, D. Stratakis, M. Babzien, S. Barber, M. Fedurin, E. Hemsing, K. Kusche, P. Muggli, B. O'Shea, X. Wei, O. Williams, V. Yakimenko, and J. B. Rosenzweig, Phys. Rev. Lett. **108**, 244801 (2012).

[10] S. Antipov, C. Jing, a. Kanareykin, J. E. Butler, V. Yakimenko, M. Fedurin, K. Kusche, and W. Gai, Appl. Phys. Lett. **100**, 1 (2012).

[11] G. Andonian, O. Williams, S. Barber, D. Bruhwiler, P. Favier, M. Fedurin, K. Fitzmorris, A. Fukasawa, P. Hoang, K. Kusche, B. Naranjo, B. O'Shea, P. Stoltz, C. Swinson, A. Valloni, and J. B. Rosenzweig, Phys. Rev. Lett. **113**, 264801 (2014).

[12] B. Naranjo, A. Valloni, S. Putterman, and J. B. Rosenzweig, Phys. Rev. Lett. **109**, 164803 (2012).

[13] E. I. Smirnova, A. S. Kesar, I. Mastovsky, M. A. Shapiro, and R. J. Temkin, Phys. Rev. Lett. **95**, 074801 (2005).

[14] B. Cowan, Phys. Rev. Spec. Top. - Accel. Beams **11**, 011301 (2008).

[15] K. Ho, C. Chan, C. Soukoulis, R. Biswas, and M. Sigalas, Solid State Comm. **89**, 413 (1994).

[16] R. J. England, R. J. Noble, K. Bane, D. Dowell, C.-k. Ng, J. E. Spencer, S. Tantawi, R. L. Byer, E. Peralta, K. Soong, B. Cowan, J. Dawson, and C. Sears, Rev. Mod. Phys. **86**, 1337 (2014).

[17] D. Grischkowsky, S. S. Keiding, M. V. Exter, and C. Fattinger, J. Opt. Soc. Am. B **7**, 2006 (1990).

[18] S. G. Joannopoulos, John D. Johnson, J. N. Winn, and R. D. Meade, *Photonic Crystals-Molding the Flow of Light*, 2nd ed. (Princeton University Press, 2008).

[19] R. E. Collin, *Field theory of guided waves*, 2nd ed. (IEEE, 1990).

[20] D. Mihalcea, P. Piot, and P. Stoltz, Physical Review Special Topics-Accelerators and Beams **15**, 081304 (2012).

[21] L. Xiao, W. Gai, and X. Sun, Physical Review E **65**, 016505 (2001).

[22] C. Jing, W. Liu, L. Xiao, W. Gai, P. Schoessow, and T. Wong, Physical Review E **68**, 016502 (2003).

[23] C. Kremers, D. N. Chigrin, and J. Kroha, Phys. Rev. A **79**, 013829 (2009).

[24] S. Johnson and J. Joannopoulos, Opt. Express **8**, 173 (2001).

[25] A. Taflove and S. C. Hagness, *Computational electrodynamics: the finite-difference time-domain method* (Artech house, 2005).

[26] `https://www.cst.com/`, accessed: 2017-11-13.

[27] A. A. Michelson and E. W. Morley, Sidereal Messenger, vol. 6, pp. 306-310 **6**, 306 (1887).

[28] A. M. Cook, R. Tikhoplav, S. Y. Tochitsky, G. Travish, O. B. Williams, and J. B. Rosenzweig, Phys. Rev. Lett. **103**, 095003 (2009).

[29] Y. Shibata, K. Ishi, T. Takahashi, T. Kanai, F. Arai, S.-i. Kimura, T. Ohsaka, M. Ikezawa, Y. Kondo, R. Kato, *et al.*, Physical Review E **49**, 785 (1994).

[30] A. Murokh, J. Rosenzweig, M. Hogan, H. Suk, G. Travish, and U. Happek, Nuclear Instruments and Methods in Physics Research Section A: Accelerators, Spectrometers, Detectors and Associated Equipment **410**, 452 (1998).

[31] N. Phinney *et al.*, *FACET-II Science Opportunities Workshops Summary Report*, Tech. Rep. (SLAC National Accelerator Laboratory (SLAC), 2016).